Discrimination of Resonant and Nonresonant Contributions to the Nonlinear Refraction Spectroscopy of Ion-Doped Solids

S. M. Lima[1] and T. Catunda[2,*]

[1]*Universidade Estadual de Mato Grosso do Sul, 79420-970, Dourados, MS, Brazil*

[2]*Instituto de Física de São Carlos, Universidade de São Paulo, 13560-970, São Carlos, SP. Brazil*

(Received 23 May 2007; published 14 December 2007)

Nonlinear refraction spectroscopy measurements were performed in resonance with absorption lines in Nd^{3+} and Cr^{3+} doped crystals. The observed line shapes can be explained by the interference of resonant and nonresonant contributions to the nonlinear refractive index. These effects were fully discriminated using a pump and probe configuration, in which a dispersive line shape was observed on the top of a plateau that was attributed to the polarizability difference between excited and ground states ($\Delta\alpha$). A theoretical model was used to obtain $\Delta\alpha$ from the experimental data, and the results are in agreement with several previous experiments. Slow and fast light propagation are also discussed.

DOI: 10.1103/PhysRevLett.99.243902 PACS numbers: 42.65.−k, 42.50.Gy, 42.55.−f

Refractive index changes are vital to understand the behavior of laser oscillators and amplifiers, particularly nonlinear behavior, pattern formation, and phase conjugate lasers [1–3]. The nonlinear properties of ion-doped materials also play an important role in the study of slow and fast light [3]. In 1966, Basov *et al.* performed experiments in ruby that motivated a discussion about fast light in amplifiers [4]. More recently, slow and fast light were observed in ruby and alexandrite absorbers [5], based on the effect of coherent population oscillations (CPO). In these experiments, a pump laser with frequency ω_1 has amplitude modulated, producing two side bands that act as probe beams with frequency $\omega_1 \pm \delta$. Since the laser pumps the metastable excited state (with lifetime $T_1 \sim$ msec), the modulation intensity at the beat frequency (δ) originates an oscillation of the population inversion. This oscillation results in a hole in the absorption spectrum, with width $\sim 1/T_1$ ($\sim 10^3$ Hz), which is $\sim$10 orders of magnitude narrower than the homogeneous linewidth. According to the Kramers-Kronig relations (KKR), this narrow spectral hole should be accompanied by a strong increase in the refractive index over the same frequency region and, consequently, low group velocity. This is also the main principle of slow light propagation obtained by electromagnetically induced transparence (EIT). Nevertheless, the results of Ref. [5] have attracted much attention because CPO does not require atomic dipole coherence [3]. Consequently, the experimental setup is very simple compared with those of EIT in vapors and solids at low temperatures. The CPO effect was then explored in several systems: Er doped fiber amplifier [6,7], semiconductors [8], bacteriorhodopsin [9], Er^{3+} doped crystals at 1.5 K [10], etc. The use of Cr^{3+} doped crystals was also proposed as temporal-nonlocal Kerr media for slow and fast light [11]. The theoretical model developed for CPO method considers the density matrix equations of motion of a saturable resonant two-level system. In fact, three- and four-level systems were used for ruby and alexandrite, respectively, but they can be reduced to the two-level case [5]. This model was later extended to explain the results of pulse propagation [12]. However, it is well-known that in a two-level system, the nonlinear refractive index ($\boldsymbol{n}_2$) has a dispersive line shape, being positive for positive detuning ($\omega > \omega_o$) and negative for $\omega < \omega_o$, a behavior not observed in ruby either at the $^4T_2$ band (centered at 555 nm) [13,14] nor at the R lines [15]. Hence, the n_2 mechanism of ion-doped solids (Cr^{3+}, Nd^{3+}, Er^{3+}) is generally attributed to nonresonant contributions originated by transitions in the UV [16–18]. The agreement obtained between theory and experiments in Refs. [5–7,12] remains a puzzle since the theoretical model contradicts numerous previous experiments involving n_2 in ion-doped materials [1,13–19]. In this Letter, we investigated n_2' and n_2'' spectroscopy of Cr^{3+} and Nd^{3+} doped crystals. Different experiments were performed in order to fully discriminate the role of resonant and nonresonant contributions for n_2. The results are in agreement with a theoretical model comprising nonresonant contributions to the susceptibility of resonant two- and three-level systems. Although KKR relations have been used to estimate $n_2'(\nu)$ from $n_2''(\nu)$, for ion-doped solids, this procedure is usually incorrect since it neglects the nonresonant term which is originated from UV transitions [20]. Furthermore, the connection between CPO and previous n_2 experiments is discussed.

In ion-doped solids (transparent crystals and glass hosts), it is generally found that the excited state has polarizability, α_{ex}, higher than that of the ground state, α_g. The contribution of the ion polarizability to the susceptibility is given by $\chi_{\mathrm{ion}} = \alpha_g N_g + \alpha_{\mathrm{ex}} N_{\mathrm{ex}}$, where $N_g(N_{\mathrm{ex}})$ is the ground (excited) state population [1]. We consider the usual case in which the system has a main excited metastable state trapping all excited state population. Therefore, in the steady state regime, the total ion concentration is

given by $N_t \sim N_{ex} + N_g$ and, consequently, $\chi_{ion} = \alpha_g N_t + \Delta\alpha N_{ex}$ where $\Delta\alpha = \alpha_{ex} - \alpha_g$ is the polarizability difference. Powell and Payne [16] observed that $\Delta\alpha(\nu)$ is always positive and increases monotonically in the IR-visible range. They explained their results in Cr^{3+} doped crystals using a single oscillator model with frequency $\sim 5 \times 10^4$ cm^{-1} that was attributed to the charge transfer bands. The $\Delta\alpha$ values of Nd^{3+} doped materials were also attributed to UV transitions, the electric dipole allowed $4f \rightarrow 5d$ transitions of rare earths [17,18]. Although these UV bands are far from resonance for visible light, they are electric-dipole allowed, so their oscillator strengths are 4 orders of magnitude greater than those of transitions in the visible. Consequently, in the context of this Letter, we call $\Delta\alpha$ a nonresonant contribution to the susceptibility ($\chi_{ion} = \chi_{nress}$). In addition to $\Delta\alpha$, the resonant contribution should be considered when the laser frequency (ω) is close to some transition frequency ω_o. This interaction is usually modeled by the two-level system (χ_{ress}) pumped by a resonant radiation field, then $N_{ex} = (N_t/2)s(1 + \Delta^2 + s)^{-1}$ where $\Delta = (\omega - \omega_o)T_2$ and $s = I/I_s$ are the normalized detuning and saturation parameters, respectively. The addition of all contributions to the susceptibility, $\chi = \chi_{nress} + \chi_{ress}$, results in

$$\chi = \chi_m + N_t\alpha_g - \frac{a_0}{2\pi k_0}\frac{i + \Delta - As}{1 + \Delta^2 + s} \qquad (1)$$

in which χ_m represents the host matrix susceptibility and $k_0 = \omega_o/c$. For $A = 0$, the term proportional to a_0 in Eq. (1) is the standard two-level system susceptibility. The effect of $\Delta\alpha$ is introduced by the parameter $A = (2\pi f_L^2 k_o/n)\Delta\alpha/\sigma_g$, in which $f_L = (n^2 + 2)/3$ is the Lorenz local field factor and σ_g is the ground state absorption cross section. Actually, Eq. (1) can be obtained from a more general expression derived by Butylkin *et al.* [21], considering that the excited state lifetime $T_1 \gg T_2$.

In this Letter, the nonlinear n_2 spectroscopy of Cr^{3+} R lines was studied using a variation of the Z-scan technique described previously [15,22], a method used here in Nd^{3+}:YAG with a cw Ti:sapphire tuned at $\sim$869 nm, the direct transition from Nd^{3+} ground to the excited metastable state ($^4I_{9/2} \rightarrow {}^4F_{3/2}$). The $n_2'(\nu)$ line shape is nearly Lorentzian and is similar to $n_2''(\nu)$, as shown in Fig. 1. This behavior is completely different from the dispersive line shapes observed in resonant interactions in four-wave mixing and EIT experiments [3,23]. Figure 1 indicates the predominance of the nonresonant contribution to χ, which follows the absorption line shape since it is proportional to $\Delta\alpha N_{ex}(\nu)$. However, a small blueshift of $n_2'(\nu)$ compared to $n_2''(\nu)$ is observed in agreement with the behavior predicted by Eq. (1) for $A \approx 1$. In fact, factor A can be directly obtained from the n_2 since that at line center ($\Delta = 0$), $A = n_2'(0)/n_2''(0) \sim 1.1$.

It is also interesting to analyze the three-level system excitation where the metastable excited state is populated

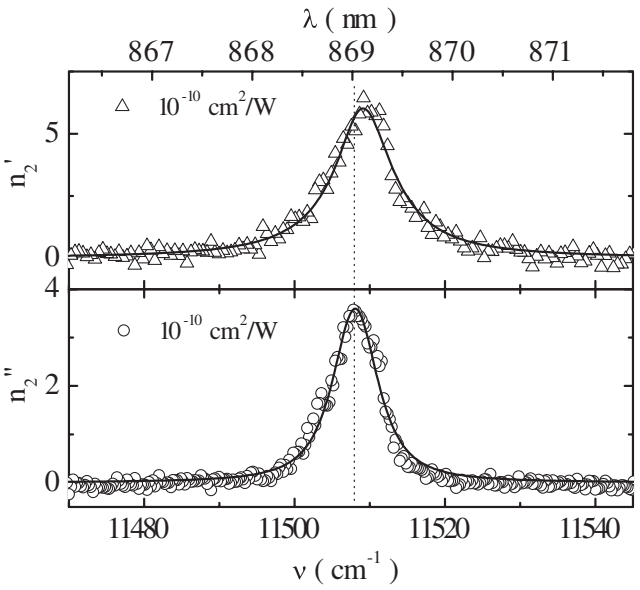

FIG. 1. $n_2(\nu)$ spectra of Nd^{3+}:YAG around the $^4I_{9/2} \rightarrow {}^4F_{3/2}$ transition. The lines are theoretical fits.

via a fast nonradiative decay from an intermediate upper state. This model is appropriate to describe the case of Nd^{3+} with 808 nm excitation, the transition from ground to the intermediate state ($^4I_{9/2} \rightarrow {}^4F_{5/2}$) which decays nonradiatively to the metastable level ($^4F_{3/2}$). Similarly to the case of ruby and alexandrite [5], this tree-level system can be reduced to a two-level one with $T_1 = \tau/2$ (where τ is the metastable level lifetime), and the resonant frequency corresponds to the energy difference between the ground and the intermediate states. Consequently, Eq. (1) can also be applied to this three-level system with the difference that factor A is 2 times larger. The $n_2(\nu)$ spectrum (not shown) obtained at 808 nm is very similar to line shape observed at 869 nm, with $n_2(0) = (2.5 - 1.4i) \times 10^{-9}$ cm^2/W indicating $A \approx 1.8$ and $\Delta\alpha = 6.0 \times 10^{-26}$ cm^3. This $\Delta\alpha$ value is in agreement with 4.6×10^{-26} cm^3 obtained by Powel *et al.* [17] from four-wave-mixing experiments. Similarly, $A \approx 1.8$ and $\Delta\alpha = 5.0 \times 10^{-26}$ cm^3 were obtained for Nd:YAP.

Figure 2 shows that the $n_2'(\nu)$ line shape changes drastically when the crystal is cooled to 150 K. With temperature decrease, linewidth of this phonon broadened transition is strongly reduced and peak absorption increased, enhancing the resonant interaction. Nevertheless, $\Delta\alpha$ and consequently the nonresonant interaction are expected to be roughly temperature independent, as observed in ruby [13]. Therefore, the dispersive line shape at $\sim$808 nm can be attributed to the decrease of the factor A with temperature decrease, since $A \propto \Delta\alpha/\sigma_g$ [Eq. (1)]. Actually, $|n_2'|$ is larger at the peak compared to the minimum, as expected for $A \sim 0.1$ [15]. However, the dispersive feature does not appear at the neighbor line at $\approx$805 nm because it has $\sigma_g \approx 13$ times smaller. In this

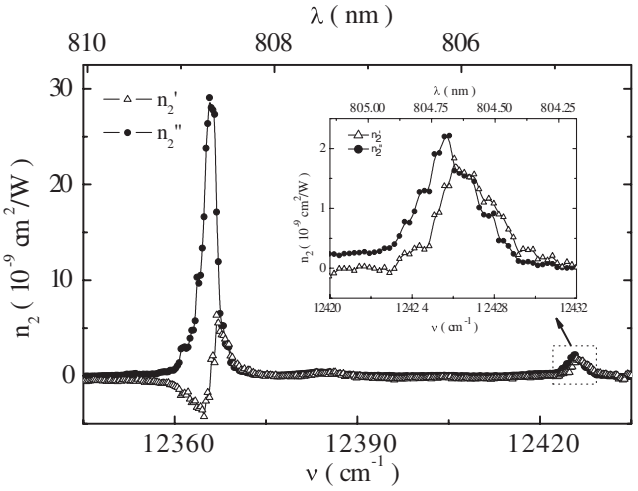

FIG. 2. $n_2(\nu)$ spectra for Nd^{3+}:YAG around the $^4I_{9/2} \rightarrow (^2H_{9/2}, ^4F_{5/2})$ transition (808 nm) at 150 K. The inset details a weaker neighbor line at $\approx$ 805 nm.

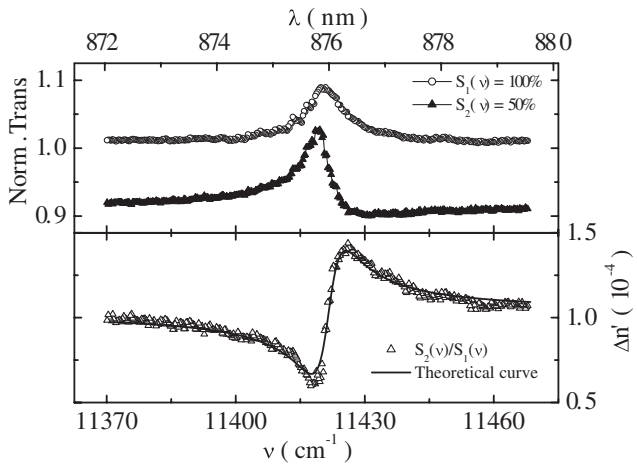

FIG. 3. The upper spectra show the closed (S_2) and opened (S_1) normalized transmittance close to 875 nm to Nd^{3+}:YAP. The lower one exhibits the expected dispersive variation of the refractive index, $\Delta n'(\nu)$, obtained by the ratio S_2/S_1. The solid line is the theoretical curve obtained as explained in the text.

case, a small blueshift of $n_2'(\nu)$ compared to $n_2''(\nu)$ can be seen, similarly to that observed in Fig. 1.

In order to properly discriminate the resonant and nonresonant contributions to n_2, two-color (pump and probe) Z-scan experiments were also performed with the purpose of obtaining the spectrum of the refractive index change (Δn_p) of a weak resonant probe beam induced by the change of excited state population (pumped by a nonresonant strong beam). A tunable Ti:sapphire laser was used as probe beam in resonance with the Nd^{3+} 869 nm transition, and an Ar^+ laser at 515 nm was chosen to pump the excited state indirectly, via nonradiative decay from upper lying levels. The sample was placed at the peak of the Z-scan curve ($z \approx 0.85 z_o$ for the probe beam) and at the pump beam focus. The top of Fig. 3 shows the signals measured in two detectors with different apertures, as described previously. The lower part of Fig. 3 shows $\Delta n_p'(\nu)$, the real part of Δn_p, which is obtained by the ratio of the two signals, $S_2(\nu)/S_1(\nu)$. A dispersive line shape is shown on the top of a background line which can be attributed to the nonresonant refractive index change proportional to $N_{ex}\Delta\alpha$. In addition, χ_{ress} is also affected by the population redistribution since a_o is proportional to $(N_g - N_{ex})$. By Eq. (1), $\Delta n_p \propto N_{ex}[A + (i + \Delta)/(1 + \Delta^2)]$ is used to fit both $\Delta n_p'$ and $\Delta n_p''$ spectra of Fig. 3, resulting in $A = 0.67$, in agreement with $A = 0.75$ determined by the single beam experiment. Similar results were obtained for Nd:YAG.

Two-color Z-scan experiments were also performed in Cr^{3+} doped crystals. An Ar^+ laser (at 515 nm) was used as excitation beam, in resonance with the $^4T_2$ band which decays to the metastable ^2E doublet. A dye laser was used as probe beam tuned to resonance with R lines of alexandrite ($\sim$680 nm). Figure 4 shows the results obtained for alexandrite with a theoretical fit performed with two A factors, one for each line, resulting in $A_1 = 2.5$ and $A_2 = 7.2$ for the R_1 line (680.2 nm) and R_2 (678.3 nm), respectively. The absorption cross section of alexandrite R_{1m} is 2.8 times larger than that of R_{2m}, in agreement with $A_2/A_1 = 2.9$, indicating that $\Delta\alpha$ is the same for both lines. Similar results were obtained for ruby R lines ($\sim$694 nm) resulting in $A_1 = 13$ and $A_2 = 20$. This kind of pump probe technique (used in Figs. 3 and 4) is much simpler than interferometric or heterodyne methods, so it has a wide range of potential applications, not only in solids, but also for Doppler free dispersion spectroscopy [3,23].

Results shown in Figs. 3 and 4 are very well fitted by the theory where the A term results in a background apparently not predicted by KKR. In fact, A results from the nonresonant contributions to $\Delta n'(\nu)$ that are neglected when KKR integral on $\Delta n''(\nu)$ is truncated (performed only on one resonant absorption). It is actually a common procedure to apply KKR in order to calculate $\Delta n'(\nu)$ from $\Delta n''(\nu)$ [20]. We demonstrated that this procedure is correct only for negligible A ($\Delta\alpha \ll \lambda\sigma$).

In order to analyze the CPO experiments of Ref. [5] and further check the validity of our model, we estimated $A = 2.7$ and $n_2' \sim 2 \times 10^{-8}$ cm^2/W were obtained for ruby at 515 nm, quite in agreement with well established experimental results [13,14]. According to this calculation, $\Delta\alpha$ accounts for $\sim$80% of n_2' value while 20% is due to the resonant interaction. In other systems, the resonant interaction can be totally dominant due to a larger absorption or emission cross section. For instance, we estimate $A \sim 0.2$ for the 1.06 μm laser transition of Nd:YAG.

In the case of CPO experiments, the population oscillation at the beat frequency δ induces a refractive index change $n(\delta)$. The modulation pattern propagates with

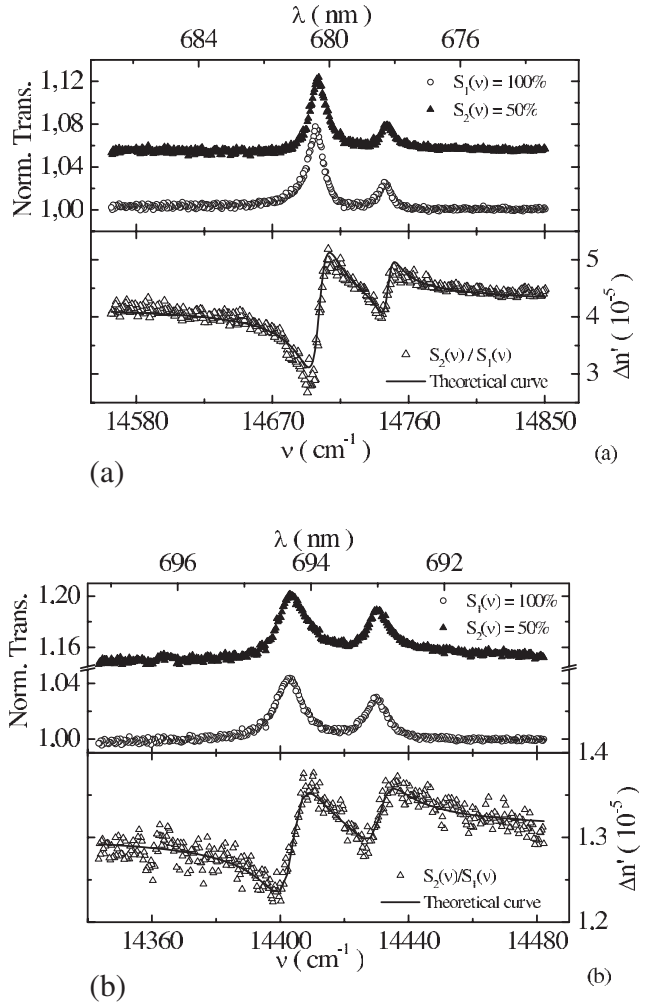

FIG. 4. Similarly to Fig. 3 for the alexandrite (a) and ruby (b) R's lines.

group index $n_{\mathrm{mod}} = n_1 + \omega_1[n(\delta) - n(-\delta)]/2\delta$, where n_1 is the refractive index experienced by the pump beam. In order to consider both resonant and nonresonant contributions, $n(\delta) = n_{\mathrm{nress}}(\delta) + n_{\mathrm{ress}}(\delta)$, we extended procedure of Ref. [5] considering the susceptibility given by Eq. (1). We noticed that n is determined only by the odd term of $n(\delta)$ which is given by $n_{\mathrm{ress}}(\delta)$. Since $n_{\mathrm{nress}}(\delta) \propto N_{\mathrm{ex}}(\delta)\Delta\alpha$ is an even function, it does not contribute to n. This cancellation effect does not appear in two-wave-mixing experiments because it involves only one side band instead of two as in CPO. Therefore, our model establishes a link between the two previously contradictory approaches of Refs. [5,11].

In conclusion, in this Letter, we studied the role of $\Delta\alpha$, which is related to the influence of all remaining levels of the system, on the resonant interactions (three or two-level system). In both cases, the role of $\Delta\alpha$ can be gauged by the parameter $A \propto \Delta\alpha/\sigma_o$. Although this effect was theoretically predicted a long time ago by Butylkin *et al.* [21], in our view, this work provides its clearest evidence. Since $A = n_2'(0)/n_2''(0)$, it is directly obtained from the experimental data. This parameter corresponds to the linewidth enhancement factor of semiconductors [8] and is important to evaluate the effects of laser-induced gratings in lasers [2]. The temperature behavior of $n_2'(\nu)$ line shape and the good agreement of the $\Delta\alpha$ data obtained from different experiments, strongly corroborate our interpretation.

*Corresponding author: tomaz@if.sc.usp.br

[1] H. J. Eichler, P. Gunter, and D. W. Pohl, *Laser-Induced Dynamic Gratings*, Spring Series in Optical Sciences Vol. 50 (Spring-Verlag, Berlin, 1986).
[2] *Phase Conjugate Laser Optics*, edited by A. Brignon and J. P. Huignard (J. Wiley & Sons, Inc., Hoboken, N. Jersey, 2004).
[3] P. W. Milonni, *Fast Light, Slow Light, Left-Handed Light, Series in Optics and Optoelectronics* (Taylor & Francis Group, New York, 2005).
[4] H. G. Basov *et al.*, Sov. Phys. JETP **23**, 16 (1966).
[5] M. S. Bigelow, N. N. Lepeshkin, and R. W. Boyd, Phys. Rev. Lett. **90**, 113903 (2003); Science **301**, 200 (2003).
[6] G. M. Gehring *et al.*, Science **312**, 895 (2006).
[7] A. Schweinsberg *et al.*, Europhys. Lett. **73**, 218 (2006).
[8] P. Ku *et al.*, Opt. Lett. **29**, 2291 (2004).
[9] P. Wu and D. V. G. L. N. Rao, Phys. Rev. Lett. **95**, 253601 (2005).
[10] E. Baldit *et al.*, Phys. Rev. Lett. **95**, 143601 (2005).
[11] Q. G. Yang *et al.*, Phys. Rev. Lett. **95**, 063902 (2005).
[12] G. S. Agarwal and T. N. Dey, Phys. Rev. Lett. **92**, 203901 (2004).
[13] C. L. Adler and N. M. Lawandy, Opt. Commun. **81**, 33 (1991).
[14] I. McMichael, P. A. Yeh, and P. H. Beckwith, Opt. Lett. **13**, 500 (1988).
[15] S. M. Lima *et al.*, Opt. Lett. **27**, 845 (2002).
[16] R. C. Powell and S. A. Payne, Opt. Lett. **15**, 1233 (1990).
[17] R. C. Powell *et al.*, Phys. Rev. B **41**, 8593 (1990).
[18] J. Margerie, R. Moncorgé, and P. Nagtegaele, Phys. Rev. B **74**, 235108 (2006).
[19] D. G. Steel and S. C. Rand, Phys. Rev. Lett. **55**, 2285 (1985).
[20] D. C. Hutchings *et al.*, Opt. Quantum Electron. **24**, 1 (1992).
[21] V. S. Butylkin, A. E. Kaplan, and Y. Khronopulo, Sov. Phys. JETP **32**, 501 (1971).
[22] M. Sheik-Bahae, A. A. Said, and E. W. Van Stryland, Opt. Lett. **14**, 955 (1989).
[23] M. Xiao *et al.*, Phys. Rev. Lett. **74**, 666 (1995).